Noise Analysis on Frequency Shifting and Filtering Algorithm-Based Phasor Estimator

Noise Analysis on Frequency Shifting and Filtering Algorithm-Based Phasor Estimator

Junhao Zhang, *Member*, *IEEE*, Lu Tang, Alessandro Mingotti, *Student Member*, *IEEE*,
Lorenzo Peretto, *Senior Member, IEEE*, He Wen, *Member, IEEE*, and Chengcheng Li

Abstract—The estimations of amplitude and phase are of great importance in the synchronous phasor measurement for power systems. In addition to the off-nominal frequency, the amplitude and phase estimations accuracy level of the power system signal is affected by the inevitable noise. In this paper, the effect of white noise on amplitude and phase estimations provided by DFT-based frequency shifting and filtering (FSF) is analysed. With the help of the Equivalent Weighting Filter's merits, viz., Equivalent Noise BandWidth and Overlap Correlation, the FSF-based amplitude and phase variance expressions are derived theoretically by considering the overlap of two processed samples. The effectiveness of the proposed amplitude and phase variance expressions are verified through computer simulations.

Index Terms—Variance analysis, Frequency shifting, Filtering, Signal to noise ratio, Cramer-Rao Lower Bound.

NOMENCLATURE

h	Order of harmonic
f_h	Frequency of hth harmonic (in herz)
A_h	Amplitude of hth harmonic (in volts)
θ_h	Phase angle of hth harmonic (in radians)
f_r	Nominal frequency (in herz)
D	Number of samples per cycle at f_r
L	Iteration times
K	Order of Equivalent Weighting Filter (EWF)
N	Number of samples
M	Measurement interval
n_1	The 1st measuring point
n_2	The 2nd measuring point
$ENBW$	Equivalent Noise BandWidth

I. INTRODUCTION

The safety and stable operation of the power systems confront challenges due to the introduction of renewable energy, as well as the development of the distributed system. Thanks to the Wide Area Measurement System (WAMS), the real-time monitoring and control level of the power system has been improved to the extent that can ensure the normal operation of the grid. As a main component of WAMS, Phasor Measurement Unit (PMU) which can provide the phasor estimation of the power systems has been developed tremendously in recent decades.

The IEEE standard C37.118.1-2011 [1], which is the widely used basis for the PMU applied in power systems in the world, stipulates that the performance of PMU is evaluated through the indicators such as Total Vector Error (TVE), Frequency Error (FE), and Rate of change of Frequency Error (RFE), etc. In addition to the influence of hardware devices, these indicators are mainly affected by the phasor estimator, including amplitude estimator, phase estimator and frequency estimator, which is the core of PMU.

Accurate phasor estimation can effectively reflect the real-time status of the power systems and provide a reliable basis for power grid protection control action. Therefore, estimating these three parameters fast and accurately has become a crucial task, which results in the proposal of several methods, e.g., the Discrete Fourier transform (DFT) [2], phase-locked loop [3], Taylor method [4], wavelet transform [5], Quasi-synchronous sampling method [6], least-square method [7], ADALINE [8], Kalman filtering [9], etc. Among them, one variant of the DFT, which is known as the Windowed Interpolation Fast Fourier transform (WIFFT), is widely spread because it well addresses the spectrum leakage and picket fence effect caused by asynchronous sampling through windowing and interpolation [10]. However, there are many data in the spectrum that are useless for the phasor estimation, which limits the efficiency of the WIFFT. In addition, the growing proportion of renewable energy sources, e.g., solar energy and wind power, requires a large number of portable low-cost monitoring devices, e.g., the micro PMUs, to provide the phasor estimations for the real-time monitoring of grid operation [11]. Thus, a more efficient phasor estimator with satisfactory performance is needed with limited computing resource and low power consumption.

The Frequency Shifting and Filtering algorithm (FSF), a

variant of DFT, estimates the frequency, amplitude, and phase of the power systems only by three steps in time domain: first, shifting the negative fundamental frequency of the sampled signal by reference signal; then, the frequency shifted signal is filtered by the iterative filtering process based on the averaging filter; finally, the parameters of the power system signal are estimated by two filtered samples [12]. In [13], the accuracy of FSF on harmonic estimation is analysed, moreover, the computational burden of FSF is reduced by using the proposed Equivalent Weighting Filter (EWF). Authors in [14] analyses the systematic error of FSF on harmonic estimation and proposes an improved FSF with systematic error compensation. As well known, the accuracy of the estimations in practical applications is not only determined by the estimator itself but also affected by the unavoidable noise introduced by the acquisition and the inherent noise [15-18]. According to [19] and [20], it is known that the inherent noise (background noise) in power system signals can be treated as white noise, and the signal-to-noise ratio (SNR) of distribution level grid signals reaches 60-70dB. [21] details the source and the principle of acquisition noise, furthermore, it analyses how the white noise affects the accuracy of frequency and ROCOF estimations in phasor measurement based on filtered heterodyned analyses. In [15] and [22], the effect of white noise on the WIFFT-based power system signal parameter estimations is analysed by deducing the variance expressions. [23] and [24] gives the variance expressions of FSF-based frequency and phase estimators according to the measurement interval to show how the estimations vary under the effect of white noise. However, the analysis of FSF-based amplitude estimation on noisy signals is still unpublished.

This paper is a technical extension of [24]. In this paper, the FSF-based amplitude and phase estimators are firstly reviewed. Then, the effect of the white noise on FSF-based amplitude and phase measurement is studied by deducing the theoretical amplitude and phase variance expressions with respect to SNR. After that, the relationship between the variance and its Cramer-Rao Lower Bound (CRLB) is analysed.

The remainder of the paper is structured as follows: Section II recalls the FSF on the power system amplitude and phase estimation. Section III analyses the influence of the white noise on FSF-based amplitude and phase estimators through the derivation of variance expressions, studies the relationship between the variances and their CRLB. Section IV provides the simulation tests and results that can verify the proposed expressions. Finally, Section V draws some conclusions.

II. AMPLITUDE AND PHASE ESTIMATION BASED ON FSF

Define $x(n)$ is a discrete signal of pure sine wave distorted by harmonics:

$$x(n) = \sum_{h=1}^{H} A_h \sin\left(\frac{2\pi f_h n}{f_s} + \theta_h\right) \qquad (1)$$

where f_h, A_h, and θ_h are the frequency, amplitude and phase angle of hth harmonic, $h=1,2,3,…,H$, H is the highest order of harmonic, $n=0,1,2,…,N-1$, N is the number of samples, f_s

represents the sampling frequency. For the power systems, f_s is set to Df_r, where D is an integer, f_r is the nominal frequency.

In practical applications, there will be a deviation Δf between nominal frequency f_r and practical fundamental frequency f_1, i.e., $\Delta f = f_r - f_1$, and it is known that $\Delta f \ll f_1$ in general.

To estimate the fundamental phasor, a reference signal $r(n)$ with frequency f_r is generated as:

$$r(n) = e^{j\frac{2\pi n f_r}{f_s}} = e^{j\frac{2\pi n}{D}}, \qquad (2)$$

where j is the imaginary unit.

Then, $x(n)$ is frequency shifted using $r(n)$ as:

$$s(n) = x(n) \cdot r(n), \qquad (3)$$

where $s(n)$ is the frequency shifted signal.

After that, $s(n)$ is filtered by the $w_{eq}(n)$ as:

$$s^L(n) = \sum_{i=n}^{K-1+n} s(i) \cdot w_{eq}(i-n+1). \qquad (4)$$

where $s^L(n)$ is the samples processed by FSF with iteration times L, $w_{eq}(n)$ represents the K-order EWF which is consisted of L averaging filters as:

$$w_{eq}(n) = \underbrace{w_A(n) * w_A(n) * \cdots * w_A(n)}_{L}, \qquad (5)$$

where $w_A(n)$ is the D-order averaging filter, "*" means the convolution operation. Thus, it can be seen that $K=L(D-1)+1$.

By virtue of frequency shifting and filtering process, the amplitude and phase of the fundamental wave are estimated by:

$$A_1 = 2 \cdot \frac{\left|s^L(n_1)\right|}{\left[G(\omega_{N-1})\right]^L}, \qquad (6)$$

$$\theta_1 = -\arg\left(V_S(n_1)\right) + \frac{\omega_{N-1} \cdot (2n_1 + K - 1)}{2} + \frac{\pi}{2}, \qquad (7)$$

where $G(\ )$ is the magnitude response of D-order averaging filter, ω_{N-1} is the sampling angular difference of fundamental negative component estimated by two samples of $s^L(n)$ as:

$$\omega_{N-1} = \frac{\arg\left(s^L(n_2)\right) - \arg\left(s^L(n_1)\right)}{M}, \qquad (8)$$

where $M=n_2-n_1$. Accordingly, the minimum number of required samples of $x(n)$ is $N=K+M$.

III. INFLUENCE OF WHITE NOISE ON FSF-BASED AMPLITUDE AND PHASE ESTIMATION

While $x(n)$ is corrupted by the white noise $z(n)$, which can be represented as:

$$y(n) = x(n) + z(n), \qquad (9)$$

where $z(n)$ is assumed to be Additive White Gaussian Noise (AWGN) with the mean and variance zero and σ^2, respectively. The SNR of $y(n)$ is defined as:

$$SNR = \frac{A_1^2}{2\sigma^2}. \qquad (10)$$

For the sake of simplicity, $s^L(n)$ in (4) is expressed by a complex vector as:

$$V_S(n) = \sum_{h=1}^{H} \left(V_{N-h}(n) + V_{P-h}(n) \right) + V_z(n), \quad (11)$$

where $V_S(n)$ is the complex vector of $s^L(n)$; $V_{N-h}(n)$ and $V_{P-h}(n)$ are the negative and the positive components of hth harmonic in $s^L(n)$ while $V_Z(n)$ is the filtered AWGN. The expressions of $V_{N-h}(n)$, $V_{P-h}(n)$, and $V_Z(n)$ are:

$$\begin{cases} V_{N-h}(n) = A_{N-h} \angle \phi_{N-h}(n) \\ A_{N-h} = \dfrac{A_h \cdot \left[G(\omega_{N-h}) \right]^L}{2} \\ \phi_{N-h}(n) = \dfrac{\omega_{N-h} \cdot (2n+K-1)}{2} - \theta_h + \dfrac{\pi}{2}, \end{cases} \quad (12)$$

$$\begin{cases} V_{P-h}(n) = A_{P-h} \angle \phi_{P-h}(n) \\ A_{P-h} = \dfrac{A_h \cdot \left[G(\omega_{P-h}) \right]^L}{2} \\ \phi_{P-h}(n) = \dfrac{\omega_{P-h} \cdot (2n+K-1)}{2} - \theta_h + \dfrac{\pi}{2}, \end{cases} \quad (13)$$

$$\begin{aligned} V_Z(n) &= B \angle \phi_Z(n) \\ &= \sum_{i=n}^{K-1+n} \left[w_{eq}(i-n+1) \cdot z(i) \cdot e^{j\frac{2\pi i}{D}} \right], \end{aligned} \quad (14)$$

where $\phi_{N-h}(n)$, $\phi_{P-h}(n)$ and $\phi_Z(n)$ represent the angle of $V_{N-h}(n)$, $V_{P-h}(n)$ and $V_Z(n)$, respectively; A_{N-h}, A_{P-h}, and B are the modules of $V_{N-h}(n)$, $V_{P-h}(n)$, and $V_Z(n)$, respectively. ω is the sampling angular frequency, and $\omega_{N-h}=2\pi(f_r-f_h)/f_s$, $\omega_{P-h}=2\pi(f_r+f_h)/f_s$.

Assume that the interferences in $V_S(n)$, i.e., $V_{N-h}(n)$ ($h=2,3,\ldots,H$) and $V_{P-h}(n)$ ($h=1,2,3,\ldots,H$), are filtered totally, thereby the only one which can lower the accuracy level is the filtered AWGN $V_Z(n)$, shown as:

$$V_S(n) \approx V_{N-1}(n) + V_z(n). \quad (15)$$

A. Derivation of the variance expressions

To analyse the effect of white noise on amplitude and phase estimations, the following characteristics of the AWGN $z(n)$ is introduced:

$$E[V_Z(n)] = 0, \quad (16)$$

$$Var[V_Z(n)] = K\sigma^2 \cdot NNPG, \quad (17)$$

where $NNPG$ is the Normalized Noise Power Gain of the EWF.

By considering the influence of $V_Z(n)$, $V_S(n)$ can be rewritten as:

$$\begin{aligned} V_S(n) &= A_S(n) \angle \eta(n) \\ &= A_{N-1} \angle \varphi_{N-1}(n) + B \angle \varphi_Z(n) \\ &= A_{N-1} \angle \varphi_{N-1}(n) \left[1 + \frac{B}{A_{N-1}} \angle \left(\varphi_Z(n) - \varphi_{N-1}(n) \right) \right], \end{aligned} \quad (18)$$

where $A_S(n)$ and $\eta(n)$ are the module and the angle of $V_S(n)$, respectively, which can be expressed as:

$$A_S(n) = A_{N-1} \left[\begin{matrix} 1 + \left(\dfrac{B}{A_{N-1}} \right)^2 \\ + \dfrac{2B}{A_{N-1}} \cos \left(\varphi_Z(n) - \varphi_{N-1}(n) \right) \end{matrix} \right]^{\frac{1}{2}}, \quad (19)$$

$$\begin{aligned} \eta(n) &= \varphi_{N-1}(n) \\ &\quad + \arctan \left[\dfrac{\dfrac{B}{A_{N-1}} \sin \left(\varphi_Z(n) - \varphi_{N-1}(n) \right)}{1 + \dfrac{B}{A_{N-1}} \cos \left(\varphi_Z(n) - \varphi_{N-1}(n) \right)} \right]. \end{aligned} \quad (20)$$

With SNR$>>$1, we know that $B/A_{N-1}<<1$. Thus, $A_S(n)$ and $\eta(n)$ can be simplified as:

$$A_S(n) \approx A_{N-1} \left[1 + \frac{2B}{A_{N-1}} \cos \left(\varphi_Z(n) - \varphi_{N-1}(n) \right) \right]^{\frac{1}{2}} \quad (21)$$

$$\eta(n) \approx \varphi_{N-1}(n) + \frac{B}{A_{N-1}} \sin \left(\varphi_Z(n) - \varphi_{N-1}(n) \right). \quad (22)$$

Applying Taylor expansion and ignoring the effects of high-order items, (21) can be simplified as:

$$A_S(n) \approx A_{N-1} + B\cos \left(\varphi_Z(n) - \varphi_{N-1}(n) \right) \quad (23)$$

Due to $\varphi_Z(n)$ is a random value in the range $[0, 2\pi]$ while $\varphi_{N-1}(n)$ and A_{N-1} are constants, according to the uncertainty propagation law [25], the variances of $\eta(n)$ and $A_S(n)$ can be expressed by the second term of (22) and (23) as:

$$Var[A_S(n)] \approx Var[B\cos \varphi_Z(n)] \quad (24)$$

$$Var[\eta(n)] \approx Var[(B/A_N)\sin \varphi_Z(n)]. \quad (25)$$

In light of Re($V_Z(n)$)=$B\cos\varphi_Z(n)$ and Im($V_Z(n)$)=$B\sin\varphi_Z(n)$, the following expression can be obtained:

$$\begin{aligned} Var[B\cos \varphi_Z(n)] &= Var[B\sin \varphi_Z(n)] \\ &= \frac{K\sigma^2 \cdot NNPG}{2} \end{aligned} \quad (26)$$

Accordingly, the variance of $A_S(n)$ is obtained as:

$$Var[A_S(n)] = \frac{K\sigma^2 \cdot NNPG}{2} \quad (27)$$

To simplify derivation of the variance, $ENBW$ of the EWF is introduced as:

$$ENBW = \frac{NNPG \cdot K^2}{\left[G(0) \right]^{2L}}. \quad (28)$$

Under the assumption $\Delta f << f_1$, $\omega_{N-1}(n) \approx 0$ can be obtained. Thereby the variance of the estimated fundamental amplitude can be deduced as:

$$\text{Var}\left[A_1\right]=4\cdot\frac{\text{Var}\left[\left|V_S(n_1)\right|\right]}{\left[G(\omega_{N-1})\right]^2}=\frac{2K\sigma^2\cdot NNPG}{\left[G(\omega_{N-1})\right]^2}$$

$$=\frac{2\sigma^2\cdot ENBW}{K}=\frac{A_1^2\cdot ENBW}{K\cdot SNR}\qquad(29)$$

As for the deduction of FSF-based phase variance, the variance of $\eta(n)$ is firstly obtained according to (12) as:

$$\text{Var}\left[\eta(n)\right]=\frac{ENBW}{K\cdot SNR}.\qquad(30)$$

By substituting (8) into (7), we can rewrite the phase estimation expression as:

$$\theta_1=\left(\frac{2n_1+K-1}{2M}\right)\arg(V_S(n_2))$$

$$-\left(\frac{2n_2+K-1}{2M}\right)\arg(V_S(n_1))+\frac{\pi}{2}.\qquad(31)$$

By replacing the first and second term of the latter equation as a and b, respectively, the variance of the phase estimation can be expressed as:

$$\text{Var}\left[\theta_1\right]=\text{Var}\left[a-b+\pi/2\right]$$

$$=\left[\text{Var}\left[a\right]+\text{Var}\left[b\right]-2\text{Cov}\left[a,b\right]\right],\qquad(32)$$

where Cov[] represents the covariance. Var[a], Var[b], and Cov[a,b] are represented as:

$$\text{Var}\left[a\right]=\left(\frac{2n_1+K-1}{2M}\right)^2\text{Var}\left[\eta(n_2)\right],\qquad(33)$$

$$\text{Var}\left[b\right]=\left(\frac{2n_2+K-1}{2M}\right)^2\text{Var}\left[\eta(n_1)\right],\qquad(34)$$

$$\text{Cov}\left[a,b\right]=\left(\frac{2n_1+K-1}{2M}\right)\left(\frac{2n_2+K-1}{2M}\right)$$

$$\cdot\text{Cov}\left[\eta(n_1),\eta(n_2)\right].\qquad(35)$$

From the previous analysis, we can see that the variance of the phase is determined by the result of Cov[$\eta(n_1)$, $\eta(n_2)$]. To analyse the Cov[$\eta(n_1)$, $\eta(n_2)$], an index of the EWF named Overlap Correlation (*OC*) [26] is introduced as:

$$OC(\delta)=\frac{\sum_{n=1}^{\delta K}\left[w_{eq}(n)w_{eq}(n+(1-\delta)K)\right]}{\sum_{n=1}^{K}\left[w_{eq}(n)\right]^2},\qquad(36)$$

where $\delta=(K-M)/K$ is the overlap coefficient. With the help of *OC*, the overlapped samples, when the weights of the EWF are different ($L>1$), are simplified as in the case of equal weights ($L=1$). Thus, the Cov[$\eta(n_1)$, $\eta(n_2)$] is approximate as:

$$\text{Cov}\left[\eta(n_1),\eta(n_2)\right]=\frac{ENBW}{K\cdot SNR}OC(\delta).\qquad(37)$$

Accordingly, the phase variance is obtained as:

$$\text{Var}\left[\theta_1\right]=\frac{ENBW}{4M^2K\cdot SNR}\left[(2n_1+K-1)^2+(2n_2+K-1)^2\right.$$

$$\left.-2(2n_1+K-1)(2n_2+K-1)OC(\delta)\right].\qquad(38)$$

B. Comparison to the CRLB

The CRLB means a lower bound for the variance of an unbiased estimator. The closer the estimator variance is to CRLB, the better the estimator is. Thus, it is necessary to analyse the relationship between the amplitude and phase variances to its CRLB. According to [25] and [27], CRLB of the unbiased amplitude and phase estimators for the sinusoidal signal are given as:

$$\text{Var}\left[A\right]_{\text{CRLB}}=\frac{2\sigma^2}{N}=\frac{A^2}{N}\cdot\frac{1}{SNR},\qquad(39)$$

$$\text{Var}\left[\theta\right]_{\text{CRLB}}=\frac{2(2N-1)}{N(N+1)}\cdot\frac{1}{SNR},\qquad(40)$$

where N is the samples used, A and θ are amplitude and phase of the sinusoidal signal. For unbiased estimation of FSF-based measurement, the interval M must be set to K at least. Here, M is fixed to K for convenience which leads to $N=2K$. Also, the amplitude of the sinusoidal signal with harmonics can be approximated to A_1. Accordingly, the CRLB of FSF-based fundamental amplitude and phase estimators thereby can be rewritten as:

$$\text{Var}\left[A_1\right]_{\text{CRLB}}=\frac{A_1^2}{2K}\cdot\frac{1}{SNR}\qquad(41)$$

$$\text{Var}\left[\theta_1\right]_{\text{CRLB}}=\frac{2}{K}\cdot\frac{1}{SNR}\qquad(42)$$

Accordingly, the relation between the FSF-based amplitude variance and its CRLB is easily obtained as:

$$\text{Var}\left[A_1\right]=\frac{A_1^2\cdot ENBW}{K\cdot SNR}=2\cdot ENBW\cdot\text{Var}\left[A_1\right]_{\text{CRLB}}\qquad(43)$$

As for the phase variance, the *OC* is 0 when $M=K$, meanwhile, n_1 is usually set to 0, thus the relationship of FSF-based phase variance and its CRLB is obtained as:

$$\text{Var}\left[\theta_1\right]=\frac{ENBW}{4K^3\cdot SNR}\left[K^2+(3K)^2\right]$$

$$=\frac{5\cdot ENBW}{2K\cdot SNR}=\frac{5}{4}\cdot ENBW\cdot\text{Var}\left[\theta_1\right]_{\text{CRLB}}\qquad(44)$$

In light of (43) and (44), it is known that the ratio of Var[A_1] and Var[A_1]$_{\text{CRLB}}$ is 2*ENBW*, while the ratio of Var[θ_1] and Var[θ_1]$_{\text{CRLB}}$ is 5*ENBW*/4.

IV. SIMULATIONS

To verify the proposed FSF-based amplitude and phase variance expressions, we firstly use a pure sinusoidal voltage signal X with frequency f_1=49.8 Hz, amplitude A_1=220 V, and phase angle θ_1=0.8 rad. Without loss of generality, each simulation result is based on 5000 independent runs. The

theoretical amplitude and phase variances are calculated by (29) and (38), respectively.
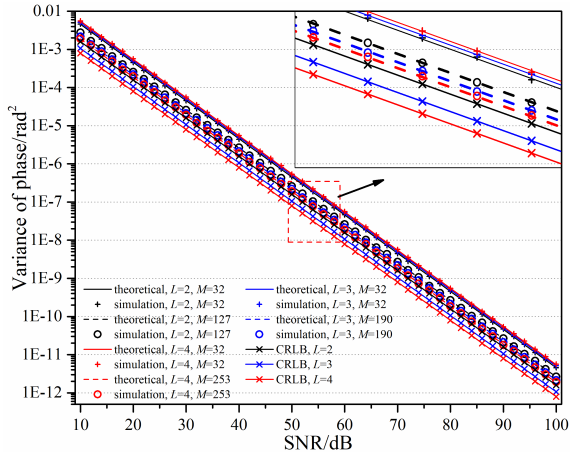
A. Influence of SNR

The sampling frequency f_s of the adopted signal X is 3.2 kHz, i.e., D=64. The measuring point n_1=0, while M is fixed to M=32 and M=K corresponding to the cases OC>0 and OC=0, respectively. The SNR of white noise added to the signal X varies from 10 to 100 dB, with 2 dB steps. The signal X is filtered for 2, 3, and 4 times. The simulation and theoretical variance results of amplitude estimations are drawn in Fig. 1, as well as the phase estimations.

Particularly, the CRLB results of the unbiased estimations are plotted in the figure to make a comparison.

Fig. 1(a) and Fig. 1(b) compares the theoretical and simulation results of amplitude and phase variances versus different SNR, respectively. As it can be seen in Fig. 1, regardless of the value of OC, the theoretical variances are consistent with the simulation one, which can confirm the correctness of the proposed variance expressions. In addition, the amplitude and phase variances are totally in inverse proportion to the SNR. The reason can be found in (29) and (38) where the SNR is a denominator of the variance expressions.
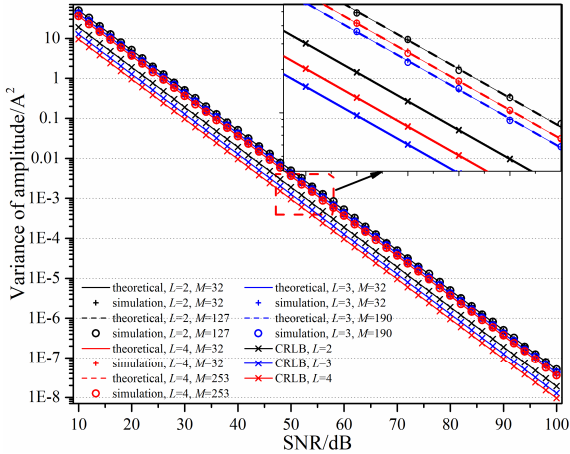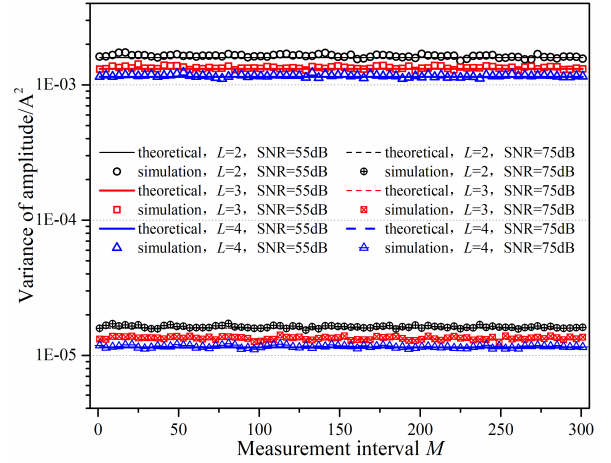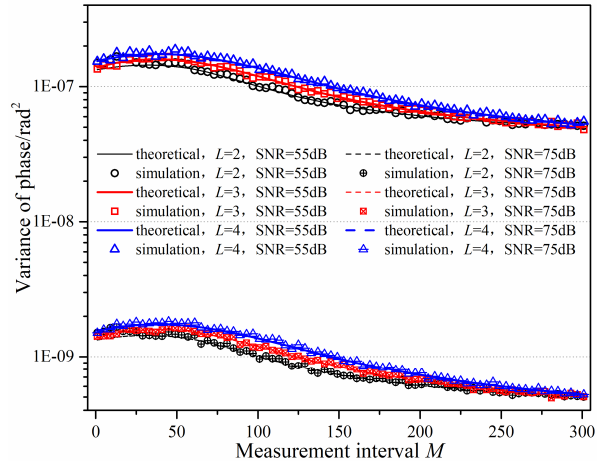

(a)

(b)

Fig. 1. Variances of the FSF-based estimations versus different SNRs, (a) amplitude variance, (b) phase variance.

(a)

(b)

Fig. 2. Variances of the FSF-based estimations versus different M and SNRs, (a) amplitude variance, (b) phase variance.

B. Influence of Number of Iterations

As the key parameter of FSF, the iteration times L determines the accuracy level, time delay, and computational efficiency of the method. As shown in (29) and (38), we can see that L can affect it through $ENBW$ and K. In addition, the phase variance also depends on OC which is an L-based parameter as well. Therefore, the effect of L on amplitude and phase variances must be evaluated. To this end, the pure signal X with SNR=75 dB is generated. The FSF is set as: D=64, n_1=0, M is selected to be M=60 (OC>0) and M=K (OC=0), L ranges from 1 to 8, N=K+M. The simulation results are listed in Table I.

According to the simulation and theoretical variance values listed in Table I, it is known that the proposed amplitude and phase variance expressions can estimate the amplitude and phase variance in actual measurements. In addition, it can be seen that the amplitude and phase variances reduce as L increases. To analyse the cause of this phenomenon, the phase variance expression (38) is simplified with the case of OC=1 as:

$$\mathrm{Var}\left[\theta_l\right] \approx \frac{ENBW}{K \cdot SNR}. \tag{45}$$

Compare (29) and (45), the same part $ENBW/(K \cdot SNR)$ can be found. In this same part, $ENBW$ is proportional to $Var[\theta_1]$ and $Var[A_1]$ while K is inversely proportional to them. On one hand, $ENBW$ corresponding to L=1, 2, 3, 4, 5, 6, 7, and 8 are 1.00, 1.32, 1.63, 1.89, 2.12, 2.32, 2.51, and 2.69, which means $ENBW$ increases as L increases. On the other hand, $K=L(D-1)+1$ is proportional to L when D is fixed. However, the increasing rate of K is larger than that of $ENBW$, which means $ENBW/K$ will reduce as L increases and this leads to the reduction of $Var[\theta_1]$ and $Var[A_1]$. The same thing can be found under the condition OC<1. However, the cost of computing resource, the measurement time delay, as well as the required number of samples, will increase if L increases.

C. Influence of Measurement Interval

According to (6) and (7), we know that the FSF-based amplitude and phase estimations are related to ω_{N-1}, which is determined by two samples of processed signal with interval M through (8). To assess the effect of M on FSF-based amplitude and phase variance, signal X with SNR=55 dB and 75 dB is generated. The measurement interval M varies from 1 to 301, with steps of 4. The iteration times L is set to 2, 3, and 4, respectively. Other parameters of FSF are n_1=0, D=64. The simulation and theoretical results are shown in Fig. 2.

As shown in the picture, the theoretical variances versus different M are consistent with the simulation ones under the same conditions, and this can validate the correctness of the proposed amplitude and phase variance expressions. Although calculating the amplitude estimation requires ω_{N-1}, the amplitude variance is independent to M. However, to the phase variance, affected by OC which is depended on M, it increases firstly and then reduces as the increment of M regardless of L. Focus on the variances with different L, we can see that when M is very small or big enough, the differences between the phase variances are quite reduced. The differences between the amplitude variances with different L are basically constant when M varies. According to these properties, if there is a high requirement for real-time measurement, it is recommended that M should be as small as possible since M directly determines the time delay of FSF.

D. Influence of Frequency Deviation and Harmonic

Frequency fluctuations and harmonics are common issues in power systems. To verify the proposed variance expressions under these influences, the pure signal X contaminated by AWGN of SNR=75dB is employed with the introductions of harmonics. The settings of the simulation are, D=64, n_1=0, M=1, L=3 and 4, the parameters of the added 2nd and 3rd harmonic are, A_2=5 V, A_3=20 V, θ_2=1.2 rad, θ_3=0.3 rad. The fundamental frequency f_1 varies from 48 Hz to 52 Hz, with a step of 0.1 Hz. The results of the simulation and theoretical variances are shown in Fig. 3.

In Fig. 3(a), we can see that, no matter the harmonics and frequency deviations, the proposed amplitude variance expression can estimate the simulation variance in [48, 52] Hz. But for the phase variance shown in Fig. 3(b), the proposed expression only valid within the range [49.5, 50.5] Hz,

frequency out of the range will leads to error between the theoretical and simulation phase variances. Same as the amplitude variance, harmonics basically have no effect on the FSF-based phase variance.

E. Simulations With Fixed Number of Samples

In many applications of the power system measurement, there will be a suggested number of signal cycles, in other words, the number of samples under fixed sampling frequency is given. Thus, to make full use of the given samples N, the values of L and M need to be tuned according to $N=L(D-1)+1+M$. In this part, signal X with f_s=2500Hz, SNR=63dB is adopted, f_1 varies from 48Hz to 52Hz by 0.4Hz-step. N is set to 250 and 400, respectively, i.e., approximately 5 cycles and 8 cycles when D=50, n_1=0, the pairs of (L,M) when N=250 can be (1,200), (2,151), (3,102), (4,53), and (5,4), the pairs of (L,M) when N=400 can be (1,350), (2,301), (3,252), (4,203), (5,154), (6,105), (7,56), and (8,7). the simulation and theoretical results are shown in Fig. 4. Besides, the Total Vector Error (TVE) results, which can represent the accuracy level of the phasor estimator, are provided.
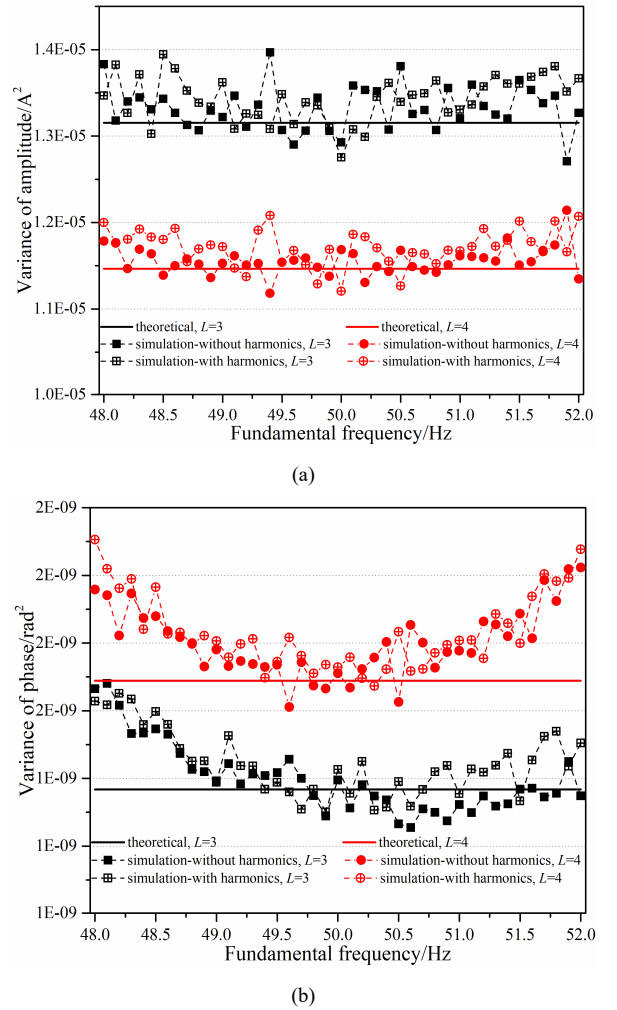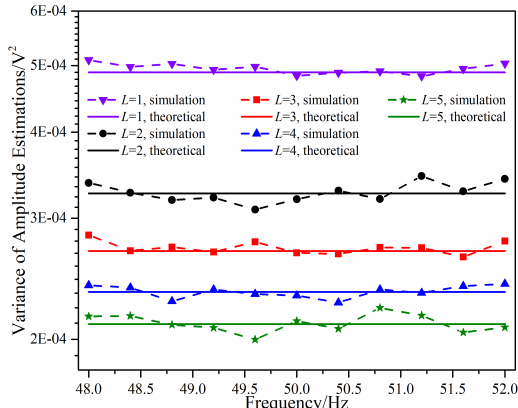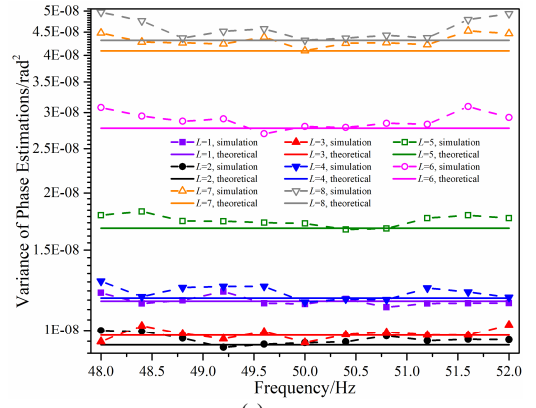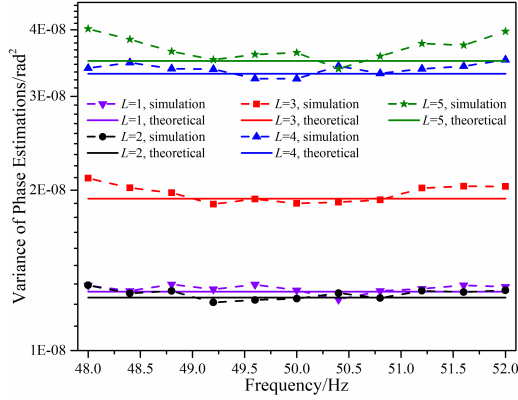

(a)

(b)

Fig. 3. Variances of the FSF-based estimations under influences of frequency deviations and harmonics, (a) amplitude variance, (b) phase variance.
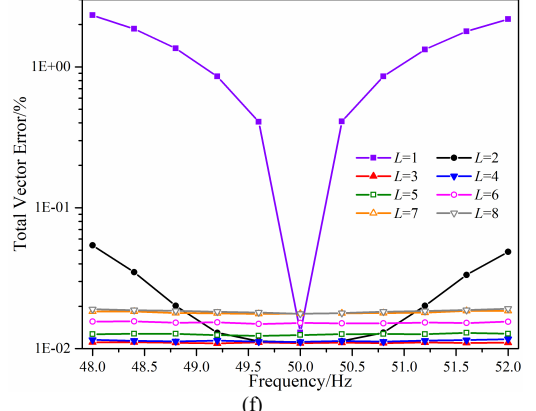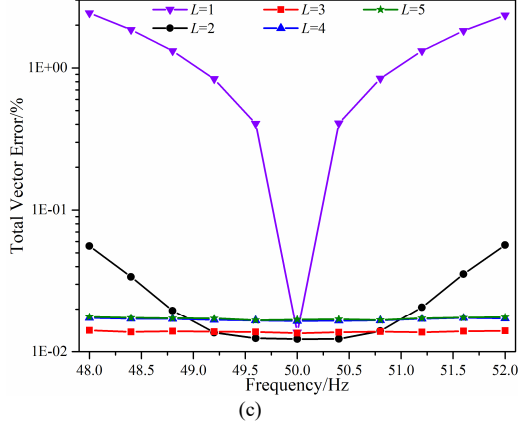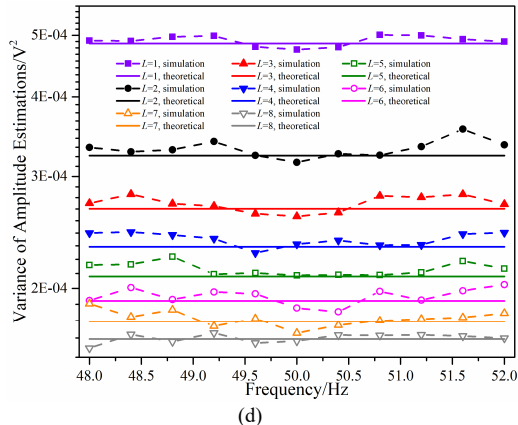
(a)

(b)

(c)

(d)

(e)

(f)

Fig. 4. Variances of the FSF-based estimations, (a) amplitude variance, N=250, (b) phase variance, N=250, (c) TVE, N=250, (d) amplitude variance, N=400, (e) phase variance, N=400, (f) TVE, N=400.

From Fig. 4, the following conclusions can be drawn: 1) the availability of the deduced variance expressions are proved by the consistency between the simulation and theoretical results. 2) the amplitude variance is independent of M, it decreases due to the increment of L, whereas the phase variance decreases first and then increases, thus, it is a tradeoff to select the combination of (L,M). The TVE can reflect the performance of the phasor measurement method including the amplitude and phase estimators. Considering the computational burden and storage requirements, according to the TVE results, the best choice is L=3 when the samples number N is fixed.

F. Simulations for Variance vs. CRLB Comparison

To verify the theoretical ratios between the FSF-based variance and its CRLB, signal X has been employed to carry out the following simulations. The settings of FSF are n_1=0, D=64, L=2, 3 and 4. The measurement interval M is set to 123, 190, and 253, respectively, to the requirement of unbiased estimation when L equals 2, 3, and 4. The simulation and theoretical ratios are listed in Table II, also the corresponding simulation variance and CRLB are provided. The theoretical ratios of amplitude and phase to their CRLB are calculated by 5$ENBW$ and 5$ENBW$/4, respectively.

As seen in Table II, the derived ratios can be used to predict the true ratios (simulation ratios). And this validates the correctness of the proposed expressions again. One thing needs

(L, M)	Simulation, $OC>0$	Theoretical, $OC>0$	(L, M)	Simulation, $OC=0$	Theoretical, $OC=0$
		Variance of amplitude estimations			
1, 60	2.35E-05	2.39E-05	1, 64	2.35E-05	2.39E-05
2, 60	1.6E-05	1.59E-05	2, 127	1.58E-05	1.59E-05
3, 60	1.29E-05	1.32E-05	3, 190	1.34E-05	1.32E-05
4, 60	1.13E-05	1.15E-05	4, 253	1.14E-05	1.15E-05
5, 60	1.04E-05	1.03E-05	5, 316	1.02E-05	1.03E-05
6, 60	9.48E-06	9.42E-06	6, 379	9.56E-06	9.42E-06
7, 60	8.91E-06	8.74E-06	7, 442	8.84E-06	8.74E-06
8, 60	8.34E-06	8.19E-06	8, 505	8.27E-06	8.19E-06
		Variance of phase estimations			
1, 60	1.32E-09	1.27E-09	1, 64	1.25E-09	1.25E-09
2, 60	1.37E-09	1.35E-09	2, 127	7.93E-10	8.28E-10
3, 60	1.57E-09	1.52E-09	3, 190	6.95E-10	6.82E-10
4, 60	1.71E-09	1.68E-09	4, 253	5.84E-10	5.94E-10
5, 60	1.83E-09	1.83E-09	5, 316	5.38E-10	5.33E-10
6, 60	1.94E-09	1.96E-09	6, 379	4.98E-10	4.87E-10
7, 60	2.07E-09	2.08E-09	7, 442	4.58E-10	4.52E-10
8, 60	2.20E-09	2.20E-09	8, 505	4.16E-10	4.23E-10

(L, SNR)	Simulation Variance	CRLB	Simulation Ratio	Theoretical Ratio
		Variance of amplitude estimations		
(2, 30)	2.69E-05	1.57E-05	1.7172	1.6538
(2, 60)	2.64E-08	1.57E-08	1.6862	1.6538
(2, 90)	2.62E-11	1.57E-11	1.6722	1.6538
(3, 30)	2.22E-05	1.05E-05	2.1188	2.0412
(3, 60)	2.17E-08	1.05E-08	2.0676	2.0412
(3, 90)	2.23E-11	1.05E-11	2.1277	2.0412
(4, 30)	1.90E-05	7.88E-06	2.4118	2.3690
(4, 60)	1.94E-08	7.88E-09	2.4640	2.3690
(4, 90)	1.89E-11	7.88E-12	2.3929	2.3690
		Variance of phase estimations		
(2, 30)	5.15E-01	1.91E-01	2.7036	2.6462
(2, 60)	4.89E-04	1.91E-04	2.5664	2.6462
(2, 90)	5.16E-07	1.91E-07	2.7066	2.6462
(3, 30)	4.16E-01	1.27E-01	3.3954	3.2660
(3, 60)	4.16E-04	1.27E-04	3.3548	3.2660
(3, 90)	4.16E-07	1.27E-07	3.2016	3.2660
(4, 30)	3.74E-01	9.57E-02	3.9065	3.7904
(4, 60)	3.58E-04	9.57E-05	3.7453	3.7904
(4, 90)	3.70E-07	9.57E-08	3.8645	3.7904

to pay attention to is that, ratio between the variances and the CRLB increases as L increases, which means the increment of L will lower the effectiveness of the FSF-based amplitude and phase estimators.

V. CONCLUSION

This paper focuses on the amplitude and phase variances by the frequency and shifting algorithm. Through the merits of the adopted Equivalent Weighting Filter, e.g., Equivalent Noise Bandwidth and Overlap Correlation, the effect of white noise on the amplitude and phase estimations is analysed theoretically by deducing the variance expressions of the amplitude and phase estimations with respect to SNR. In light

of the proposed expressions, the FSF-based phase variance is inversely proportional to SNR as well as the amplitude variance. Meanwhile, it is shown that the amplitude and phase variances are influenced by the iteration times and the sampling frequency. The difference is that the phase variance depends on the measurement interval while the amplitude variance not. In addition, according to the given simulation results, this paper suggests that the optimal choice of the iteration times under the condition of a fixed measurement period is 3.

REFERENCES

[1] *IEEE Standard for Synchrophasor Measurements for Power Systems*, 2011.

[2] D. Belega and D. Petri, "Accuracy of the Synchrophasor Estimator Returned by the Interpolated DFT Algorithm Under Off-Nominal Frequency and Harmonic Conditions," in *2018 IEEE 9th International Workshop on Applied Measurements for Power Systems (AMPS)*, 2018, pp. 1-6: IEEE.

[3] A. Cataliotti, V. Cosentino, and S. Nuccio, "A phase-locked loop for the synchronization of power quality instruments in the presence of stationary and transient disturbances," *IEEE Transactions on Instrumentation and Measurement,* vol. 56, no. 6, pp. 2232-2239, 2007.

[4] M. A. Platas-Garza and J. A. de la O Serna, "Polynomial implementation of the Taylor–Fourier transform for harmonic analysis," *IEEE Transactions on instrumentation and measurement,* vol. 63, no. 12, pp. 2846-2854, 2014.

[5] W.-K. Yoon and M. J. Devaney, "Power measurement using the wavelet transform," *IEEE Transactions on Instrumentation and Measurement,* vol. 47, no. 5, pp. 1205-1210, 1998.

[6] X. Dai and R. R. Gretsch, "Quasi-synchronous sampling algorithm and its applications," *IEEE Transactions on Instrumentation and Measurement,* vol. 43, no. 2, pp. 204-209, 1994.

[7] I. Sadinezhad and V. G. Agelidis, "Real-time power system phasors and harmonics estimation using a new decoupled recursive-least-squares technique for DSP implementation," *IEEE Transactions on Industrial Electronics,* vol. 60, no. 6, pp. 2295-2308, 2013.

[8] G. W. Chang, C.-I. Chen, and Q.-W. Liang, "A two-stage ADALINE for harmonics and interharmonics measurement," *IEEE Transactions on Industrial Electronics,* vol. 56, no. 6, pp. 2220-2228, 2009.

[9] C. Huang, X. Xie, and H. Jiang, "Dynamic Phasor Estimation Through DSTKF Under Transient Conditions," *IEEE Transactions on Instrumentation and Measurement,* vol. 66, no. 11, pp. 2929-2936, 2017.

[10] H. Wen, J. Zhang, Z. Meng, S. Guo, F. Li, and Y. Yang, "Harmonic estimation using symmetrical interpolation FFT based on triangular self-convolution window," *IEEE Transactions on Industrial Informatics,* vol. 11, no. 1, pp. 16-26, 2015.

[11] P. K. Dash and S. Hasan, "A Fast Recursive Algorithm for the Estimation of Frequency, Amplitude, and Phase of Noisy Sinusoid," *IEEE Transactions on Industrial Electronics,* vol. 58, no. 10, pp. 4847-4856, 2011.

[12] J. Zhang, W. He, T. Lu, Z. Teng, and C. Zhou, "Frequency Shifting And Filtering Algorithm for Power System Harmonic Estimation," in *IEEE International Workshop on Applied Measurements for Power Systems*, 2017.

[13] Z. Shuai, J. Zhang, L. Tang, Z. Teng, and H. Wen, "Frequency shifting and filtering algorithm for power system harmonic estimation," *IEEE Transactions on Industrial Informatics,* vol. 15, no. 3, pp. 1554-1565, 2018.

[14] J. Zhang, H. Wen, and L. Tang, "Improved Smoothing Frequency Shifting and Filtering Algorithm for Harmonic Analysis with Systematic Error Compensation," *IEEE Transactions on Industrial Electronics,* vol. 66, no. 12, pp. 9500-9509, 2019.

[15] D. Belega, D. Petri, and D. Dallet, "Influence of wideband noise on sinusoid parameter estimation provided by the two-point interpolated odd-DFT algorithm," in *2016 12th IEEE International Symposium on Electronics and Telecommunications (ISETC)*, 2016, pp. 293-297: IEEE.

[16] A. Mingotti, L. Peretto, and R. Tinarelli, "Uncertainty Analysis of an Equivalent Synchronization Method for Phasor Measurements," *IEEE Transactions on Instrumentation and Measurement,* vol. 67, no. 10, pp. 2444-2452, 2018.

[17] L. Peretto, R. Sasdelli, and R. Tinarelli, "Uncertainty propagation in the discrete-time wavelet transform," *IEEE transactions on Instrumentation and Measurement,* vol. 54, no. 6, pp. 2474-2480, 2005.

[18] H. Wen, L. B. Kish, A. Klappenecker, and F. Peper, "New noise-based logic representations to avoid some problems with time complexity," *Fluctuation & Noise Letters,* vol. 11, no. 02, p. 1250003, 2012.

[19] Z. Jin and H. Zhang, "Noise characteristics and fast filtering of synchronized frequency measurement in low voltage grid," in *2016 IEEE Smart Energy Grid Engineering (SEGE)*, 2016, pp. 398-403.

[20] H. Wen, C. Li, and W. Yao, "Power System Frequency Estimation of Sine-Wave Corrupted With Noise by Windowed Three-Point Interpolated DFT," *IEEE Transactions on Smart Grid,* vol. 9, no. 5, pp. 5163-5172, 2018.

[21] A. J. Roscoe, S. M. Blair, B. Dickerson, and G. Rietveld, "Dealing With Front-End White Noise on Differentiated Measurements Such as Frequency and ROCOF in Power Systems," *IEEE Transactions on Instrumentation and Measurement,* vol. 67, no. 11, pp. 2579-2591, 2018.

[22] C. Offelli and D. Petri, "Weighting effect on the discrete time Fourier transform of noisy signals," *IEEE transactions on Instrumentation and Measurement,* vol. 40, no. 6, pp. 972-981, 1991.

[23] J. Zhang, L. Tang, A. Mingotti, L. Peretto, and H. Wen, "Analysis of White Noise on Power Frequency Estimation by DFT-based Frequency Shifting and Filtering Algorithm," *IEEE Transactions on Instrumentation and Measurement,* pp. 1-1, 2019.

[24] J. Zhang, L. Tang, A. Mingotti, L. Peretto, H. Wen, and C. Li, "Effect of White Noise on Phase Estimation by Frequency Shifting and Filtering Algorithm," in *2019 IEEE 10th International Workshop on Applied Measurements for Power Systems (AMPS)*, 2019, pp. 1-6.

[25] S. M. Kay, *Fundamentals of statistical signal processing*. Prentice Hall PTR, 1993.

[26] F. J. Harris, "On the use of windows for harmonic analysis with the discrete Fourier transform," *Proceedings of the IEEE,* vol. 66, no. 1, pp. 51-83, 1978.

[27] C. Offelli and D. Petri, "The influence of windowing on the accuracy of multifrequency signal parameter estimation," *IEEE Transactions on Instrumentation and Measurement,* vol. 41, no. 2, pp. 256-261, 1992.

Junhao Zhang (S'17, M'20) was born in Henan, China, in 1986. He received the B.Sc. and Ph.D. degrees from Hunan University in 2009, and 2019, respectively. He is currently working as a Postdoc in the College of Electrical and Information Engineering, Hunan University, Hunan, China. His research interests include electrical measurement, digital signal processing, and calibration of instrument transformers.

Lu Tang received his B.Sc. and M.Sc. degree from Huazhong University of Science and Technology, and his Ph.D degree from Academy 0f Mathematics and Systems Science, Chinese Academy of Sciences (CAS). Since 2007, he has been a Lectuer in Hunan University, his main interest and research field are power system analysis, signal processing and complex systems.

A. Mingotti (S'17) was born in Cento (FE), Italy in 1992. He received the B.S. and the M.S. degrees in electrical engineering from the University of Bologna (Italy), in 2014 and 2016, respectively. He is currently pursuing the PhD degree in biomedical, electrical, and system engineering at the University of Bologna under the supervision of Prof. Lorenzo Peretto. His research interests include management and condition maintenance of distribution networks, development, modelling, and metrological characterization of instrument transformers.

L. Peretto (M'98, SM'03) is a Professor of Electrical and Electronic Measurements at the University of Bologna, Italy. He is Senior Member of IEEE and member of the IEEE Instrumentation and Measurement Society. He is Chairman of the annual IEEE Applied Measurements for Power System Conference, member of the IEC TC38 "Instrument Transformers" and Chairman of the TC38/WG45 "Standard Mathematical Models for Instrument Transformers" and of the TC38/WG53 "Uncertainty evaluation in the calibration of Instrument Transformers".

His fields of research are the design and calibration of voltage and current instrument transformers (LPIT) for medium and high voltage power networks; the design and realization of calibration systems of voltage and current instrument transformers; measurements of electrical quantities in power networks.

He is author and co-author of more than 200 papers and of 24 patents and co-author of three books. He is consultant of industries operating in the field of instrumentation and sensors for electrical measurements.

He Wen (M'12) was born in Hunan, China, in 1982. He received the B.Sc., M.Sc, and Ph.D. degrees in electrical engineering from Hunan University, Hunan, China, in 2004, 2007, and 2009, respectively. He is currently a full professor with the College of Electrical and Information Engineering, Hunan University, China. His present research interests include electrical contact reliability, wireless communications, power system harmonic measurement and analysis, power quality, and digital signal processing. Also, he is the deputy director of Hunan Province Key Laboratory of Intelligent Electrical Measurement and Application Technology.

He is an Associate Editor of the IEEE TRANSACTIONS ON INSTRUMENTATION AND MEASUREMENT, and a Member of Editorial Board of FLUCTUATION AND NOISE LETTERS.

Chengcheng Li received the B.Sc. degree from Zhejiang Sci-tec University in 2015. She is currently working toward the Ph.D. degree in the College of Electrical and Information Engineering, Hunan University, Hunan, China. Her research interests include electrical measurement and digital signal processing.